SiC Diffractive Waveguides for Augmented Reality: Single-Layer, Full-Color, Rainbow-Artifact-Free Display with Vision Correction

Boqu Chen[1,2], Ce Li[3], Xiaoxuan Li[1], Chenting Fang[3], Yinggang Chen[4], Ding Zhao[3], Lu Cai[4*], Kaikai Du[3,4*] and Min Qiu[1,3,5*]

[1]. Zhejiang Key Laboratory of 3D Micro/Nano Fabrication and Characterization, Department of Electronic and Information Engineering, School of Engineering, Westlake University, 18 Shilongshan Road, Hangzhou 310030, Zhejiang Province, China.

[2]. College of Information Science and Electronic Engineering, Zhejiang University, Hangzhou 310007, Zhejiang Province, China

[3]. Westlake Institute for Optoelectronics, Fuyang, Hangzhou 311421, Zhejiang Province, China.

[4]. Moldnano (Hangzhou) Technology Co., Ltd., Hangzhou 311100, Zhejiang Province, China.

[5]. Institute of Advanced Technology, Westlake Institute for Advanced Study, 18 Shilongshan Road, Hangzhou 310024, Zhejiang Province, China.

Supplementary Information

Full color display diffractive waveguide technical roadmap comparison

A systematic comparison of representative full-color display technologies employing diffractive waveguides is presented in Table S1, encompassing prior work, this work, Meta Orion, Magic Leap, Microsoft HoloLens, and achromatic metagrating waveguide. Current diffractive waveguide architectures for augmented reality (AR) displays predominantly rely on high-refractive-index glass paired with index-matched nanoimprint resist. This material combination offers advantages in low-cost fabrication and scalable manufacturing processes. However, inherent limitations in refractive indices (< 2.0) for both glass and resin necessitate multilayer waveguide stacking to achieve full-color performance, resulting in increased device thickness and compromised wearability. For instance, Magic Leap's six-layer waveguide (~2 mm) and Microsoft HoloLens' three-layer waveguide (~1.5 mm) exemplify the trade-offs between optical functionality and ergonomic design.

Recent progress in achromatic metagrating waveguides has demonstrated single-layer full-color displays through duty-cycle-modulated Si_3N_4 gratings on glass substrates, significantly improving luminance uniformity. Despite these advancements, challenges persist in mass production due to the stringent requirements for subwavelength structure aspect ratios and broad-range duty-cycle modulation, limiting current implementations to prototype stages.

The emergence of silicon carbide (SiC) diffractive waveguides has marked a pivotal shift in AR display technology. Initial breakthroughs were independently reported in September 2024 through prior work and the Meta Orion prototype. The latter system, designed as a high-performance demonstrator, utilizes a single-layer dual-side SiC waveguide to achieve 70° field-of-view (FOV) full-color projection. While optically promising, its complex fabrication process lacks publicly verifiable scalability.

In prior work, SiC diffractive waveguides were first introduced for AR applications, achieving three critical milestones: single-layer full-color display with integrated vision correction capabilities, ultra-thin packaging (30 μm) addressing weight-volume constraints, and rainbow artifact suppression through strategic stray-light redirection. Subsequent structural optimizations in the current methodology have yielded a RGB display luminance efficiency of 1238.10 nit/lm and brightness uniformity of 20.45%, enabling bright and clear display. Notably, the current solution has transitioned to mass production, with cost projections derived from manufacturing datasets offering practical guidance for industry adoption.

This progression establishes a framework for balancing optical performance, ergonomic design, and industrial scalability in next-generation AR displays, addressing long-standing challenges in optical performance, form factor, and production viability.

Table S1: Full Color Display Diffractive Waveguide Technical Roadmap Comparison

Feature	Prior work[1]	This work	Meta Orion[2]	Magic Leap[3]	Microsoft Hololens[4]	Achromatic metagrating[5]
Release Date	2024.09.24	-	2024.09.26	2017.12.21	2015.01.22	2025.4.30
Waveguide Material	SiC	SiC	SiC	High index glass & resist	High index glass & resist	Si_3N_4 on glass
Waveguide Layer	1 (Single side)	1 (Single side)	1 (Dual side)	6	3	1 (Single side)
Thickness	0.55 mm	0.75 mm	Unknown	2 mm	1.5 mm	0.5 mm
Field of View (FOV)	30°	30.82°	70°	50°	34°	20°
Luminance Effiency (RGB display)	175.45 nit/lm	1238.10 nit/lm	Unknown	220 nit (Light engine luminance unknown)	320 nit (Light engine luminance unknown)	Unknown
Brightness Uniformity (RGB display)	3.18 %	20.45 %	Unknown	Unknown	Unknown	15.23 % (Centre)
Distortion	1.48 %	1.52%	Unknown	Unknown	Unknown	Unknown
Rainbow Artifacts Elimination	Yes	Yes	Unknown	No	No	No
Vision Correction Integration	Yes	Yes	Unknown	No	No	No
Packaging Method	Hard coating (30 μm)	Hard coating (30 μm)	Cover glass (millimeter scale)	Cover glass (millimeter scale)	Cover glass (millimeter scale)	No
Technical Phase	Mass production	Mass production	Demo	Mass production	Mass production	Demo
Mass Production Unit Cost	< 500 dollars	< 500 dollars	Unknown	> 3000 dollars	> 2000 dollars	Unknown

Simulation of diffraction efficiency across functional regions

To evaluate the diffraction efficiency in each functional region, simulations were performed across the field of view (FOV), and the results are illustrated in Figure S1. The input coupler (IC) region exhibits relatively high diffraction efficiency; however, losses accumulate as the number of total internal reflections (TIR) increases during light propagation, causing a decrease in overall performance. Consequently, the diffraction efficiencies in the exit pupil expansion (EPE) and out coupler (OC) regions continue to diminish. Because blue light has a shorter wavelength, it undergoes more TIR, leading to a lower diffraction efficiency in the OC region. Conversely, red light has a longer wavelength and thus fewer TIR, resulting in a higher final diffraction efficiency for the OC region. These findings are consistent with the actual experimental results.

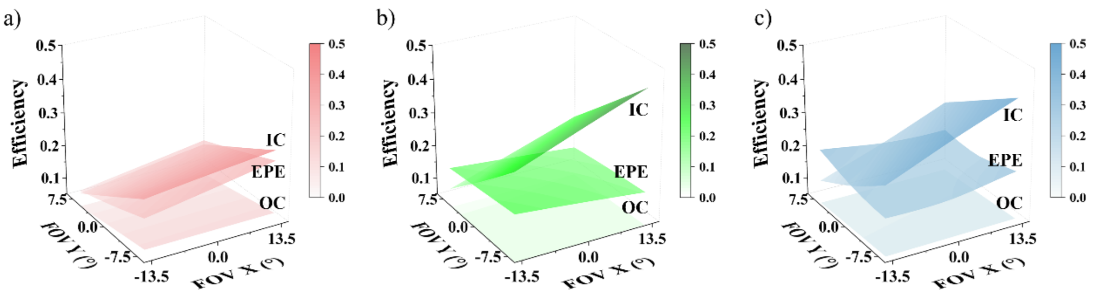

Figure S1. Diffraction efficiency of each functional region. (a) Diffraction efficiency of SiC waveguide at 635 nm within the FOV. **(b)** iffraction efficiency of SiC waveguide at 528 nm within the FOV. **(c)** Diffraction efficiency of SiC waveguide at 463 nm within the FOV.

Simulation of material refractive index with FOV limit

Based on the same single-layer RGB display, the same substrate thickness and structure processability range and other design indexes, the upper limit of waveguide device FOV design for different refractive index substrates is compared by simulation calculation. The maximum FOV is directly related to the refractive index of the substrate. The maximum diagonal FOV is given by Equation 1:

$$\theta_{FOV} = 2\sin^{-1}(\frac{n_w - n_{air}}{2}) \quad (1)$$

where n_w and n_{air} are the refractive index of substrate and air, respectively. According to the method provided in the literature, the refractive index of SiC substrate in the visible range is approximately 2.62@532 nm, which corresponds to a FOV range of about 80° for a single layer full-color waveguide. For traditional glass, the maximum refractive index is around 2.0@532 nm, leading to a FOV range about 35° for a single layer full-color waveguide. The Figure S2 illustrates the maximum FOV that the waveguide can support under these two conditions.

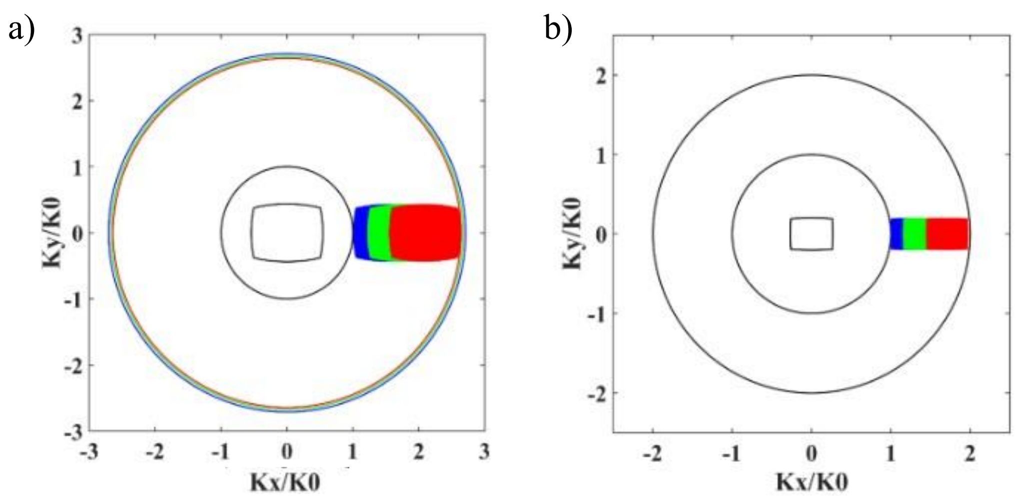

Figure S2. Theoretically maximum FOV supported by single layer waveguide with full color display. (a) SiC waveguide with 80° FOV. **(b)** 2.0 Refractive index glass waveguide with 35° FOV.

Reliability Testing of Ultra-Thin Packaging

Comprehensive reliability testing was conducted to evaluate the mechanical strength, stability, and durability of ultra-thin packaging methods. As illustrated in Figure S3a, the mechanical strength test follows the ball drop test method outlined in the GB 10810-1996 standard. A ball drop impact tester is used to vertically drop a 43 g steel ball with a 22 mm diameter from a height of 1.3 m onto a SiC waveguide surface placed flat on the testing platform. After the impact, the sample showed no deformation or damage on its surface, indicating compliance with the mechanical strength standard for the device.

For stability assessment, the test utilized the high-low temperature cycling method described in section 5.3.2 of the GB/T 12085.2-2022 standard, at a severity level of 9, as shown in Figure S3b. Samples were placed in a rapid temperature change chamber, with test conditions including low temperature (-65°C), high temperature (85°C), storage duration of 2.5 hours, transition rate (0.2–2 K/min), and five cycles. Following the high-low temperature cycling test, the samples exhibited no deformation or damage, demonstrating compliance with the stability standard for the device.

To evaluate durability, the testing protocol employed the xenon lamp aging method specified in ASTM G155-2021, as shown in Figure S3c. SiC waveguides were placed in a xenon lamp aging chamber featuring a light source with an irradiance of 0.35 W/(m²·nm) at 340 nm, chamber temperature maintained at 43°C, and a relative humidity of 50%. The test procedure consisted of 102 minutes of light exposure followed by 18 minutes of combined light exposure and spraying, repeated 12 times for a total of 24 hours. Upon completion of the xenon lamp aging test, the samples remained free from discoloration or deformation, confirming compliance with the durability standard for the device.

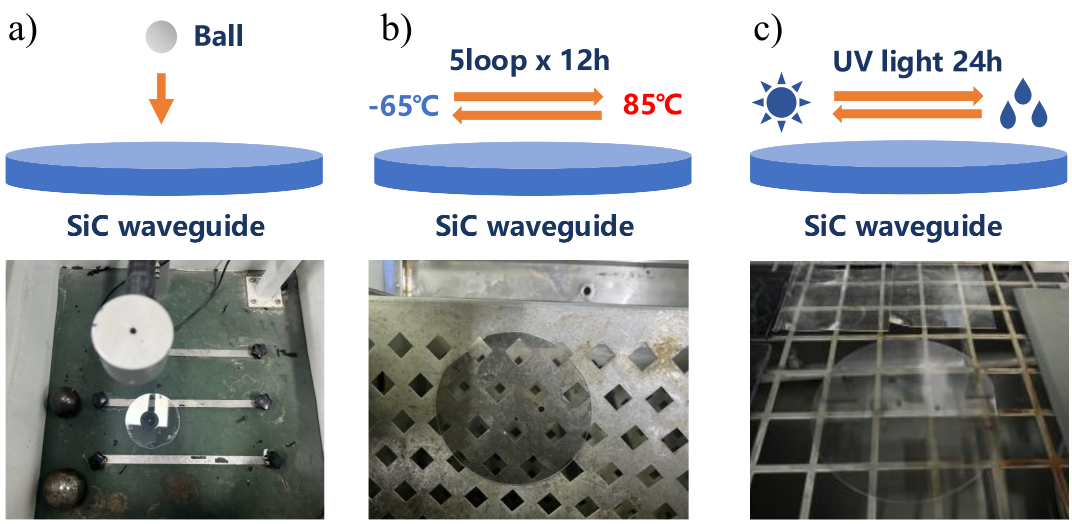

Figure S3. Schematic and experimental illustrations of ultra-thin packaging reliability tests. (a) Ball drop test. **(b)** High-low temperature cycling test. **(c)** Xenon lamp aging test.

FOV Compatibility

The SiC waveguide is specifically optimized for a 30° FOV to achieve maximum efficiency within this range, as shown in Figure S4a. However, variations in optical engine designs and models result in practical FOVs that can extend beyond the design specifications when integrated with the

SiC waveguide. As illustrated in Figure S4b, for optical engines with a maximum display FOV of 50°, the SiC waveguide can support an effective FOV of up to 46°, due to the inherently high refractive index of the SiC material. In practical applications, the optical engine is matched to the optimal design parameters of the SiC waveguide to ensure optimal display performance.

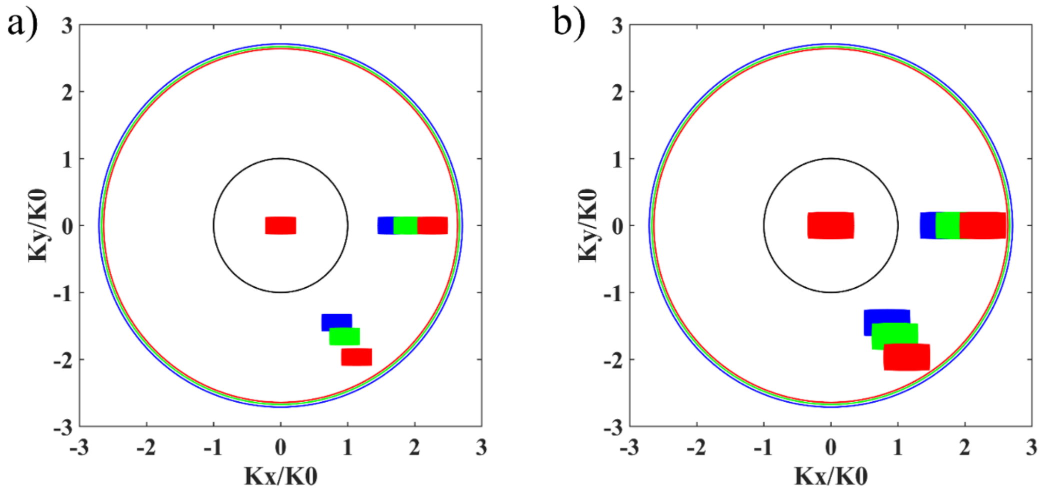

Figure S4. Simulation results of FOV compatibility. (a) The k-space diagram corresponding to a 30° FOV. **(b)** The k-space diagram corresponding to a 46° FOV.

Optical performance test

The test methodology is based on international electrotechnical commission (IEC) eyewear display standard: IEC 63145-20-20. To evaluate the luminance uniformity of the SiC waveguide under RGB mixed, red, green, and blue light, we utilized a custom-built optical testing platform. The light engine and luminance colorimeter were precisely aligned to the centers of the SiC waveguide's input coupler (IC) and output coupler (OC) regions, respectively, with the focus adjusted until the image appeared sharp. The relative spatial arrangement is depicted in Figure S5. A total of 25 test points were distributed across the eye-box region, and the luminance at each point was measured using the array sensor of the luminance colorimeter. The brightness uniformity U within the eye-box region was calculated using Equation 2, where L_{E1} to L_{E25} represent the luminance values of the individual test points.

$$U = \frac{\min(L_{E1}, L_{E2}, \ldots, L_{E25})}{\max(L_{E1}, L_{E2}, \ldots, L_{E25})} \quad (2)$$

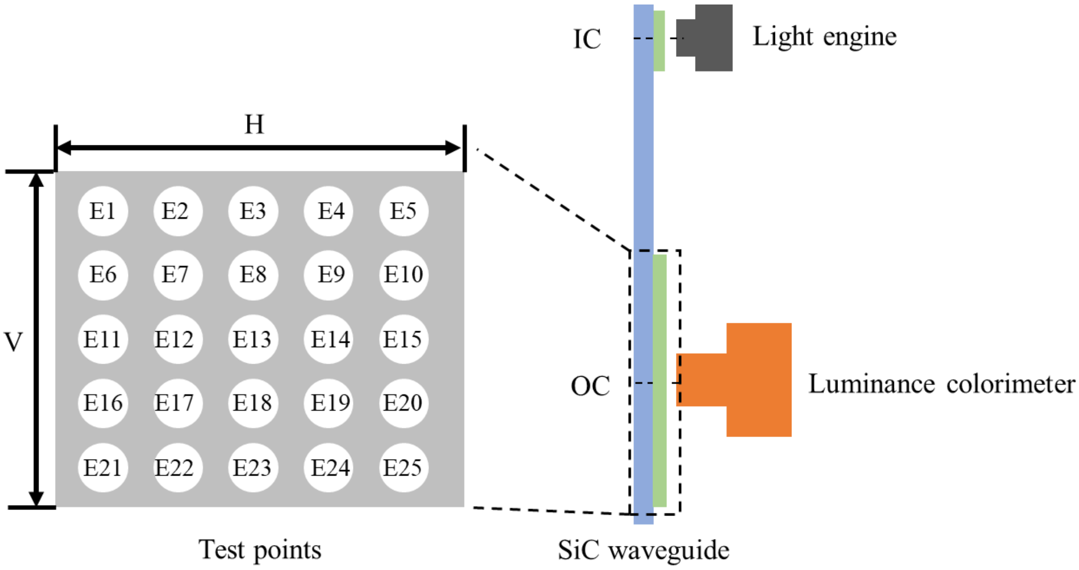

Figure S5. Schematic of the optical testing setup and the distribution of test points.

Luminance values L_{E1} to L_{E25}) at each test point within the OC region were obtained using a luminance colorimeter. The average luminance (L_{avg}) was calculated using Equation 3. The luminance of the optical engine output (A) was measured by aligning the luminance colorimeter directly with the optical engine. The luminous efficiency (η) was then calculated using Equation 4. These steps were repeated under RGB mixed, red, green, and blue conditions to obtain the respective results.

$$L_{avg} = \frac{L_{E1} + L_{E2} + \cdots + L_{E25}}{25} \tag{3}$$

$$\eta = \frac{L_{avg}}{A} \tag{4}$$

Display clarity was evaluated using the Michelson contrast as the metric. A test chart consisting of line pairs with varying pixel widths was used, with the field of view and pixel density converted to a resolution of 11 lp/deg. Horizontal and vertical test charts were measured using a luminance colorimeter, and the Michelson contrast score ($C_{m.i}$) was calculated based on Equation 5, where $L_{vM,i}$ and $L_{vm,i}$ represent the maximum and minimum luminance in the image, respectively.

$$C_{m.i} = \frac{L_{vM,i} - L_{vm,i}}{L_{vM,i} + L_{vm,i}} \tag{5}$$

To assess distortion, a 10×10 grid of light spots was projected using the optical engine, and the resulting grid in the OC region was captured using the luminance colorimeter. The distortion metric (δ_{vh}) was computed using Equation 6, where $A_{m,vh}$ and $A_{i,vh}$ denote the measured and ideal semi-diagonal angles, respectively.

$$\delta_{vh} = \frac{A_{m,vh} - A_{i,vh}}{A_{i,vh}} \tag{6}$$

Rainbow Artifacts Test

To simulate potential rainbow artifacts issues arising from ambient light interactions with the SiC waveguide under daily usage conditions, a custom rainbow artifacts testing platform was designed and assembled. As illustrated in Figure S6a, tests were conducted by varying the light source position and the rotational angle of the SiC waveguide. The test conditions consisted of combinations of light source angles at 0°, 30°, 60°, and 80°, and sample rotation angles at 0°, 30°, 60°, 90°, 120°, 150°, 180°, 210°, 240°, 270°, 300°, 330°, and 360°, resulting in a total of 37 test configurations. A luminance colorimeter was aligned with the central OC region and positioned 15 mm away at the eye relief distance, simulating a human eye FOV of 70° × 46°. A total of 195 measurement points were recorded, and the results are displayed in Figure S6b.

The experimental configuration included both transmission and reflection test arrangements, as illustrated in Figures S6c and S6d. The experimental setup was mounted on a vibration-isolated optical platform within a darkroom environment. The system consisted of a movable diffuse light source (114493.95 nit), a luminance colorimeter, and a rotatable sample holder. During the transmission tests, the average stray light intensity across all FOVs was 19.21 nit, with a single FOV stray light generation ratio of 0.02%. Similarly, during the reflection tests, the average stray light intensity across all FOVs was 19.51 nit, with a single FOV stray light generation ratio of 0.02%.

The testing results demonstrated the SiC waveguide's exceptional capability to suppress rainbow artifacts across various angles, providing a significant advancement in optical performance for AR display devices.

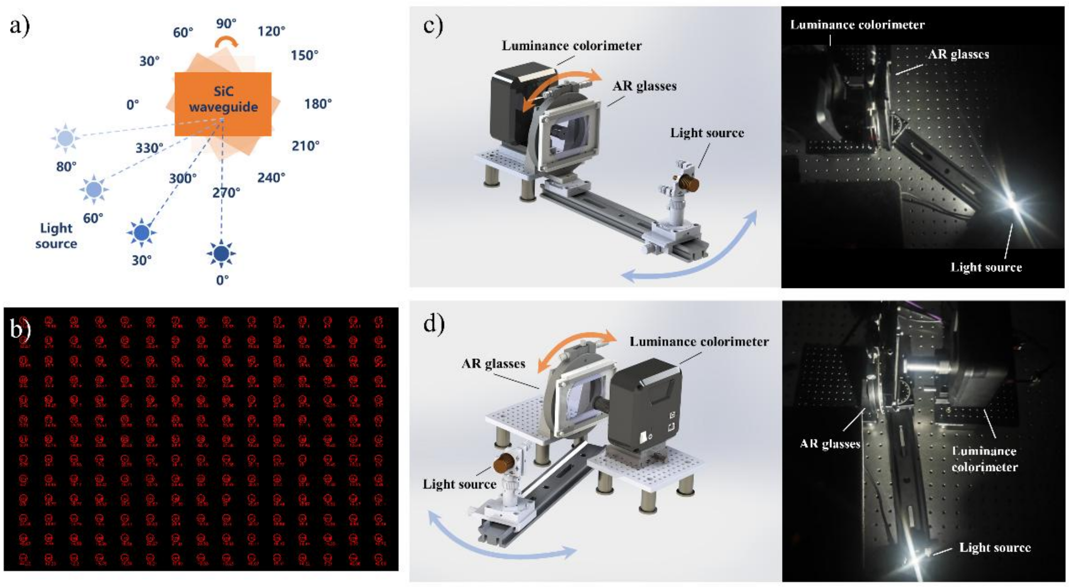

Figure S6. Schematic and experimental illustrations of rainbow artifacts test. (a) Ambient light testing angle configurations. **(b)** Luminance colorimeter measurement points (marked in red). **(c)** Transmission rainbow artifacts test schematic and setup. **(d)** Reflection rainbow artifacts test schematic and setup.

Cost Estimation for Mass Production

At present, the growth process for 4-inch SiC wafers is relatively mature and cost-effective. Based on the actual production of 300 pieces of 4-inch with 2-unit SiC waveguides, cost projections were made for future large-scale production of 8-inch SiC wafers at monthly outputs of 5000 and

20000 units. According to industry development trends, 8-inch SiC wafers are expected to offer advantages in cost, structural utilization efficiency, and feasibility for mass production. With 8-inch SiC wafers, each wafer can accommodate 8 waveguide units. As Figure S7 shows, for monthly production of 5000 SiC waveguide units, the unit cost is approximately 900 RMB. When the production volume increases to 20000 units, the unit cost decreases to 651 RMB.

In the mass production of SiC waveguides, the dominant cost factor is the material cost of SiC wafers, and this cost proportion does not decrease significantly with increased production volume. In the coming years, as the semi-insulated SiC wafer growth process is optimized and production scales up, the substrate material cost is expected to decrease rapidly, potentially driving further reductions in the overall cost of SiC waveguides.

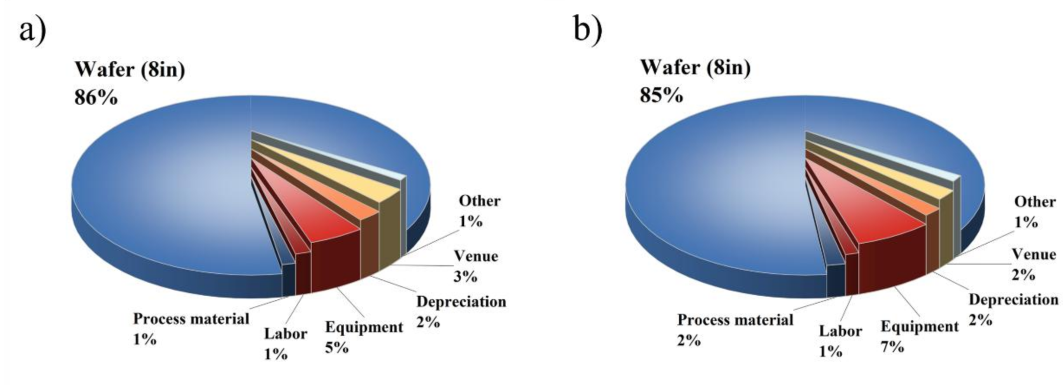

Figure S7. Cost distribution analysis for mass production of SiC waveguides. (a) 5k units/month production scenario. **(b)** 20k units/month production scenario.

References

1 Chen, B. *et al.* Ultra-Thin, Ultra-Light, Rainbow-Free AR Glasses Based on Single-Layer Full-Color SiC Diffrcative Waveguide. *arXiv preprint arXiv:2409.14487* (2024).

2 *Meta. Orion AI Glasses: The Future of AR Glasses Technology*, <https://about.meta.com/realitylabs/orion/>

3 Yeoh, I. L., Edwin, L. E. & Macnamara, J. G. (Google Patents, 2020).

4 Kress, B. C. & Cummings, W. J. in *SID symposium digest of technical papers.* 127-131 (Wiley Online Library).

5 Moon, S., Kim, S., Kim, J., Lee, C.-K. & Rho, J. Single-layer waveguide displays using achromatic metagratings for full-colour augmented reality. *Nature Nanotechnology*, 1-8 (2025).